Image-Guided Intensity-Modulated Radiotherapy for Pancreatic Carcinoma

Martin Fuss, Adrian Wong, Clifton D. Fuller, Bill J. Salter, Cristina Fuss, Charles R. Thomas, Jr.

ABSTRACT

Purpose: To present the techniques and preliminary outcomes of ultrasound-based image-guided intensity-modulated radiotherapy (IG-IMRT) for pancreatic cancer.

Materials and Methods: Retrospective analysis of 41 patients treated between November 2000 and March 2005 with IG-IMRT to mean total doses of 55 Gy (range, 45-64 Gy). We analyzed the clinical feasibility of IG-IMRT, dosimetric parameters, and outcomes, including acute gastrointestinal toxicity (RTOG grading). Survival was assessed for adenocarcinoma (n = 35) and other histologies.

Results: Mean daily image-guidance corrective shifts were 4.8 ± 4.3 mm, 7.5 ± 7.2 mm, and 4.6 ± 5.9 mm along the x-, y-, and z-axes, respectively (mean 3D correction vector, 11.7 ± 8.4 mm). Acute upper gastrointestinal toxicity was grade 0–1 in 22 patients (53.7%), grade 2 in 16 patients (39%), and grade 3 in 3 patients (7.3%). Lower gastrointestinal toxicity was grade 0–1 in 32 patients (78%), grade 2 in 7 patients (17.1%), and grade 4 in 2 patients (4.9%). Treatment was stopped early in 4 patients following administration of 30 to 54 Gy. Median survival for adenocarcinoma histology was 10.3 months (18.6 months in patients alive at analysis; n = 8) with actuarial 1- and 2-year survivals of 38% and 25%, respectively.

Conclusion: Daily image-guidance during delivery of IMRT for pancreatic carcinoma is clinically feasible. The data presented support the conclusion that safety margin reduction and moderate dose escalation afforded by implementation of these new radiotherapy technologies yields preliminary outcomes at least comparable with published survival data.

Gastrointest Cancer Res 1:2–11. © 2007 by International Society of Gastrointestinal Oncology

M. Fuss, MD: Department of Radiation Oncology, The University of Texas Health Science Center at San Antonio, Texas, the Cancer Therapy & Research Center, San Antonio, and the Department of Radiation Medicine, Oregon Health & Science University, Portland, OR

A. Wong, BA: Department of Radiation Oncology, The University of Texas Health Science Center at San Antonio, TX

C.D. Fuller, MD: Department of Radiation Oncology and Division of Radiological Sciences, The University of Texas Health Science Center at San Antonio, TX

B.J. Salter, PhD: Department of Radiation Oncology, University of Utah, Salt Lake City, UT

C. Fuss, MD: Department of Radiology, The University of Texas Health Science Center at San Antonio, TX

C.R. Thomas, Jr., MD: Department of Radiation Medicine, Oregon Health & Science University, Portland, OR

Recent advances in the planning and delivery of radiotherapy, including intensity-modulated radiotherapy (IMRT), have facilitated improved tumor-conformal radiation dose delivery.[1] Individualized steep radiation dose gradients between tumor or target volumes and adjacent normal tissues are readily enabled. This permits, at least theoretically, the ability to escalate radiation doses to the tumor while maintaining, or even reducing, normal tissue exposure, hence increasing the therapeutic ratio in gastrointestinal (GI) tumor radiotherapy.[2,3]

In radiotherapy for pancreatic cancer, adequate dose delivery to target tissue is hampered by the radiosensitivity of normal adjacent structures. The proximity of organs at risk poses an obstacle to optimal dose distribution and disappointing median and long-term survival rates. Accordingly, efforts to develop more effective treatments and improve outcomes have included studies of radiation dose escalation and/or concurrent chemotherapy intensification.[4,5] To facilitate radiotherapy intensification using advanced, highly conformal dose delivery, planning target volume (PTV) safety margins (which, by definition, consist entirely of normal tissues at risk for radiotoxicity) must be reduced.

Image-guided radiotherapy (IGRT) is a recent conceptual development that permits daily assessment of a target's position relative to the linear accelerator beam geometry, thus enabling correction of positional setup errors. Therefore, the component of the PTV safety margin assigned to offset the effects of interfraction setup variability may be effectively reduced.

In this report, we summarize our preliminary clinical experience in implementing daily ultrasound-based image guidance into courses of IMRT for pancreatic cancer. To our knowledge, no data exist in the literature regarding the implementation of image guidance with IMRT for

Address correspondence to: Martin Fuss, MD, Department of Radiation Medicine, Oregon Health & Science University, 3181 SW Sam Jackson Park Rd., L337, Portland, OR 97239. Phone: 513-494-8758; Fax 503-494-6967; E-mail: fussm@ohsu.edu.

pancreatic cancers. Thus, the purpose of this article is to provide an overview of this treatment technique and an evaluation of its clinical feasibility. Preliminary clinical outcomes, including treatment-related toxicity and overall survival, are reported.

MATERIALS AND METHODS

Chart review, data collection, and data analysis were approved by the Institutional Review Board (IRB) of The University of Texas Health Science Center at San Antonio under IRB protocol #E-012-112 and E-034-023.

Patient and Tumor Characteristics

Between November 2000 and March 2005, 41 patients aged 17 to 83 years (mean, 61 years; median, 59 years) completed a course of adjuvant or definitive image-guided serial tomotherapeutic IMRT for pancreatic cancer. Patient characteristics, tumor stage, nodal and metastatic status, as well as surgical and chemotherapy regimens employed are summarized in Tables 1 and 2.

Preradiotherapy Surgical Management

Seventeen patients (41%) underwent a total or subtotal resection of their tumor prior to radiotherapy. Of those, 13 patients (76.5%) underwent a Whipple procedure, and four (23.5%) underwent partial pancreatectomy. Complete tumor resection with negative histopathologic margins was achieved in 11 patients (65%). Positive surgical margins were confirmed in pathology specimens from 6 patients (35%) (Table 2).

Computed Tomography (CT) Simulation

Planning image data were obtained via helical scanning technology on a clinical treatment simulation platform. Image data were acquired with patients in the supine position, without the use of immobilization devices, during normal, relaxed, free breathing. Image data were reconstructed in sequential 2.5mm or 3.0mm slices. Administration of a timed bolus infusion of non-ionic intravenous contrast media afforded excellent visualization of vascular structures. No oral contrast was administered to avoid introducing stomach and small bowel filling not reproduced throughout the course of treatment.

Since all simulation imaging data in the present cohort were acquired before the availability of four-dimensional computed tomography (4D CT) capabilities, additional inhale/exhale CT scans were acquired to estimate the range of tumor and organ motion. Alternatively, a simulator CT mounted digital fluoroscopy unit was used to assess breathing motion.

IMRT Planning and Delivery

Radiotherapy planning and delivery technologies included CORVUS® inverse IMRT treatment planning software, MIMiC® serial tomotherapy delivery, and BAT®

volume/tumor bed, plus the entire circumference of the duodenum and nodal drainage areas, including pancreaticoduodenal nodes, celiac axis nodes, superior mesenteric artery nodes, and the porta hepatis (peripancreatic nodes were partially included) or areas of positive margins post resection. For dose prescription, the CTVi was expanded into an initial planning target volume (PTVi) by adding margins of 10 mm (median, 10 mm; range 10–15 mm). Target volumes in patients with tumors confined to the pancreatic body and pancreatic tail lesions (9 of 41 patients) differed in that the entire circumference of the duodenum was not included in the initial target volume.

Table 1: Patient demographics and tumor characteristics.

Characteristic		n
Mean age (range)	59 years (17–83 years)	
Gender	Male	31
	Female	10
Ethnicity	White	22
	Hispanic	14
	Black	4
	Asian	1
TNM staging	T1N0M0	1
	T2N0M0	2
	T2N1M0	1
	T2N2MX	1
	T3N0M0	5
	T3N1M0	11
	T3N1M1	1
	T4N0M0	4
	T4N1M0	13
	T4N1M1	2
Histology	Adenocarcinoma	35
	Islet cell tumor	1
	Neuroendocrine	1
	Neuroectodermal	1
	Indeterminate	3
Location	Head	30
	Body	5
	Tail	4
	Ampullary	2

ultrasound image-guided localization technology (North American Scientific/ Nomos, Cranberry Township, PA).

After transferring image data into the Corvus® treatment planning software, the clinical target volume (CTV) was delineated. Also, organs at risk, including the spinal cord, kidneys, and liver, were delineated.

The initial CTV (CTVi) for pancreatic head lesions included the gross tumor

In 31 patients, a planned boost was delivered to a reduced target volume, which typically encompassed the gross tumor volume. For pancreatic head lesions, the inner aspect of the duodenum was included in the boost CTV (CTV$_{boost}$). The CTV$_{boost}$ was extended by expanding safety margins from 6 mm to 10 mm (median, 6 mm) into a PTV$_{boost}$. Prescribed doses to the PTVi ranged from 41.4–60.4

Gy (median, 46 Gy) in daily doses of 1.8 to 2 Gy. Median prescription doses to the PTV$_{boost}$ were 14 Gy (range, 4–18 Gy) in conventional fractionation. Median cumulative total dose prescription to PTV and PTV$_{boost}$ was 54 Gy (mean, 55 Gy; range, 45–64 Gy). Dose and volume parameters are summarized by cohort in Table 3.

Using an inverse IMRT planning system, dose prescription required definition of the desired target goal dose, the percentage of target volume allowed to receive lesser doses (typically set to no more than 3%), the minimum dose to be received by the target volume (95% of prescribed dose), and the maximum allowed target dose (approximately 107% of prescribed dose). Similarly, dose limits for organs at risk, percentages of organs at risk allowed to receive more than the specified dose limit, and minimum and maximum allowed doses to organs at risk were defined (Figure 1). Since serial tomotherapeutic IMRT uses a rotational or arc method of delivery, a range of gantry rotation was specified (340°, rotation from 350° to 10°).

The MIMiC® binary multileaf beam collimator, which is used specifically for this type of IMRT, provides two collimator inherent pencil beam dimensions of 8.5×10 mm (1 cm mode) and 17×10 mm (2 cm mode). Treatments were planned and delivered using the 2 cm pencil beam mode in 39 patients. In two patients, both the initial treatment as well as the boost were computed and delivered using the 1 cm mode. Treatment plans were subsequently optimized using a simulated annealing inverse-planning approach. Typical resulting dose distributions for an initial plan and boost volume are shown in Figure 2.

Treatments were delivered using a 6 MV linear accelerator with 400 or 600 monitor unit (MU)/min dose-rate delivery capability through the attached MIMiC binary multileaf collimator. The median number of couch indices required for the slice-by-slice serial tomotherapeutic IMRT approach ranged from 3–7 (median, 4) and 2–6 (median, 3) for the PTVi and the PTV$_{boost}$, respectively.

Table 2: Treatment characteristics: surgery and chemotherapy.

Treatment	Cohort	n
Surgery	No surgery	24
	Surgery performed	17
	Pancreaticoduodenectomy	13
	Partial pancreatectomy	4
Surgical outcome	Complete gross resection	11
	Positive disease margins	6
Chemotherapy	Capecitabine	17
	5-FU	10
	5-FU/gemcitabine	1
	Gemcitabine/cisplatin	2
	Gemcitabine	4
	Vincristine/ifosfamide/etoposide	1
	Irinotecan	1
	No chemotherapy	5

Ultrasound-Based Image Guidance

To generate anatomical structures for export to the BAT® ultrasound-based image-guidance system, the simulation CT dataset was copied after target tissue and organs at risk had been delineated for inverse IMRT planning. In addition to organ outlines already established, vessels (aorta, major named arteries, vena cava, and venous structure of the extrahepatic portal vein system) and surgically placed clips in close anatomical relation to the CTV were identified. These "guidance structures" were individually delineated with regard to specific anatomical morphology and tumor location, with feasibility of ulstrasound visibility as a primary consideration.

The structure sets were electronically transferred into the image-guidance system

and a "BAT study," consisting of five anatomical structures (a technical limitation inherent to the system), was generated. In a typical scenario, a BAT study structure set consisted of the aorta with major named arteries (celiac trunk and superior mesenteric artery), vena cava, the extrahepatic portal vein system (superior mesenteric vein, lienal vein, confluens, portal vein), the liver, and the gross tumor volume, surgical clips, or biliary stent (Figure 3).

The concept and workflow of ultrasound-based image guidance using the BAT system has been previously reported.[6–11] Before delivery of each IMRT fraction, the patient was positioned supine upon the treatment couch and fiducial skin marks were aligned with room lasers. Transabdominal ultrasound images were acquired in approximately axial and sagittal planes. Computed-tomography-delineated target and guidance structure outlines were then superimposed onto the actual real-time ultrasound imaged anatomy (Figure 3). Second to user initiated virtual shifts of the CT-derived structure set to match the actual ultrasound anatomy, the system

Table 3: Radiation plan dosimetric parameters.

Cohort	n	Total Prescription Dose (Gy) Median (Range)	PTVi (cm³) Median±SD	PTVi Dose (Gy) Median (Range)	PTV$_{boost}$ (cm³) Median±SD	PTV$_{boost}$ (Gy) Median (range)
All	41	54 (45–64)	927.6±440.1	46 (41.4–60.4)	371.8±258.8	14 (4–18)
Locally advanced	24	59.4 (45–64)	961.2.5±483.1	46 (41.4–60.4)	354.7±238.8	11 (4–18)
Adjuvant	17	54 (45–64)	868.9±383.6	46 (45–50.4)	436.1±304.5	8 (4–18)
R0 resection	6	52.2 (45–60)	778.9±312.2	48 (45–50.4)	532.2±136.5	8 (6–14)
R1 resection	11	54 (50–64)	1028.2±418.8	46 (46–50.4)	340.8±364.4	8 (4–18)

Target Name		Type	Goal (Gy)	Vol Below Goal (%)	Min (Gy)	Max (Gy)	I
Target1 – target		Homogenous	46.0	3	43.5	50.0	☐

Dose prescription to PTVi

Sensitive Structure Name		Type	Limit (Gy)	Vol Above Limit (%)	Min (Gy)	Max (Gy)	I
Tissue		Homogenous Tis	46.0	0	0.0	46.0	☐
Kidney (L)		Basic Structure	16.0	35	14.0	46.0	☐
Kidney (R)		Basic Structure	16.0	35	14.0	46.0	☐
Spinal Cord		Basic Structure	30.0	10	25.0	40.0	☑

Target Name		Type	Goal (Gy)	Vol Below Goal (%)	Min (Gy)	Max (Gy)	I
Target1 – target		Homogenous	14.0	3	13.5	18.0	☐

Dose prescription to PTV$_{boost}$

Sensitive Structure Name		Type	Limit (Gy)	Vol Above Limit (%)	Min (Gy)	Max (Gy)	I
Tissue		Homogenous Tis	14.0	0	0.0	14.0	☐
Kidney (L)		Basic Structure	5.0	33	2.0	8.0	☐
Kidney (R)		Basic Structure	5.0	33	2.0	8.0	☐
Spinal Cord		Basic Structure	10.0	10	9.0	12.0	☐

Figure 1: Typical intensity-modulated radiotherapy (IMRT) dose prescription for initial (upper screen) and boost planning target volume (PTV) (lower screen).
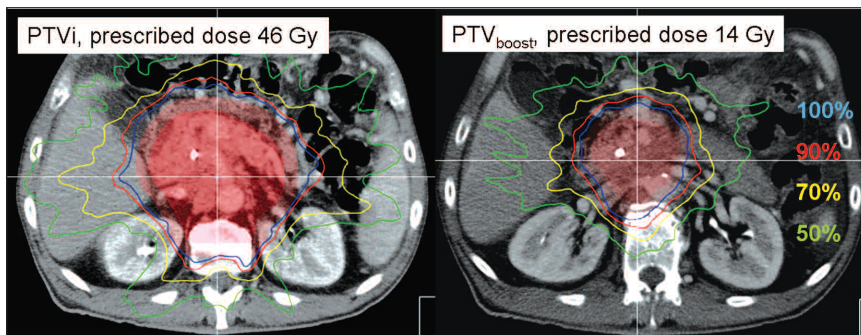

Figure 2: IMRT dose distribution for initial planning target volume (PTVi) and PTV boost. Displayed are the 100% (blue), 90% (red), 70% (yellow), and 50% (green) isodose lines. The respective clinical target volumes and PTVs are shaded in light tones of red to allow anatomy display.

reports the corresponding required correctional shifts along the primary room axes. Following execution of these suggested shifts, a confirmatory ultrasound image set was acquired to assure anatomical alignment.

Chemotherapy

Concurrent with radiotherapy, 33 patients (80.5%) received chemotherapy; the specific chemotherapy regimens are listed in Table 2. Five patients did not receive concurrent chemotherapy (12.2%). Three patients received neoadjuvant chemotherapy prior to surgical resection and adjuvant radiotherapy only (7.3%).

Statistical Analysis

Demographic data were collected, including patient age, gender, ethnicity, histologic classification, chemotherapy regimen, TNM staging, and surgical resection. Dosimetric parameters analyzed included the CTV and PTV volumes and radiation dose. Also, mean dose exposure of liver, kidneys, and spinal cord were recorded. We correlated organ-at-risk dose with volume of CTV and PTV, as well as total radiation dose prescribed, in a linear regression analysis. We did not attempt to derive dosimetry data for small bowel radiation exposure owing to the fact that the entire duodenal loop was part of the

initial target volume for the majority of patients and that the boost volume still included a significant part, typically the inner aspect, of the duodenal C-loop. It is important to note that the simulation CT scan provides only a snapshot-in-time spatial representation of the small bowel, and the potential for positional change to occur over the course of radiation delivery is significant.

Toxicity analysis, specifically GI toxicity, was performed using the Radiotherapy Oncology Group's (RTOG) acute toxicity scales as grading criteria. Gastrointestinal toxicity was assessed in two categories—upper GI toxicity, and lower GI toxicity. Upper GI toxicity included, nausea, vomiting, anorexia, and abdominal pain. Lower GI toxicity included changes in bowel habits, diarrhea, abdominal distension, GI bleeding, perforation, fistula, or tenesmus. To calculate an estimate for the probability for normal tissue toxicity, logistic regression analysis correlated CTV and PTV volume, as well as total prescribed dose, with maximally observed toxicity according to RTOG grading.

Survival data were collected and analyzed for patients with adenocarcinoma histopathology using Kaplan-Meier actuarial analysis. Pathologies other than adenocarcinoma were excluded from this analysis since the different biologic behavior of these tumors probably outweighs any treatment-related effects. Survival was calculated from date of pathologic diagnosis as well as from start of radiotherapy for inoperable patients. In patients who underwent attempted curative resection of their disease prior to adjuvant radiotherapy, the date of surgery was the basis for survival analysis.

RESULTS

Image Guidance

In 39 patients for whom all shift data were available, a total of 1,011 image-guidance attempts were electronically recorded. Individually, 15 to 35 (median, 28) image-guidance attempts were performed. Shift data for two patients could not be obtained, because the data storage media could not be accessed for one and data were lost during transfer to a central archive drive for the other. Average absolute corrective

shifts indicated by the BAT system were 4.8 ± 4.3 mm (mean ± standard deviation), 7.5 ± 7.2 mm, and 4.6 ± 5.9 mm along the x-, y-, and z-axes, respectively. The average length of the 3D magnitude vector of positional correction was 11.7 ± 8.4 mm. Three-dimensional corrective shifts larger than 10, 15, and 20 mm were executed in 49.9%, 27.0%, and 13.5% of targeting attempts. The magnitude of shifts in the principal directions as well as the 3D vector of displacement was significant (test against the zero hypotheses) at $P<.0001$ (Figure 4).

In two patients, corrective shifts at the initiation of treatment were consistently in excess of 25 mm along at least one principal axis. A re-simulation CT scan revealed dramatic changes in stomach and bowel filling between simulation and treatment start, as documented in Figure 5. In both instances, a new treatment plan was generated. Consequently, image-guidance derived corrective shifts were reduced to the average range of the cohort.

Plan Dosimetry

Prescribed total doses ranged from 45 to 64 Gy (median, 54 Gy; mean, 55 Gy). In patients who received their treatment in two phases (n = 31), the median initial dose prescribed was 46 Gy, with an additional median boost dose of 14 Gy.

The average CTVi and PTVi volumes were 561.71 ± 318.7 and 1003.6 ± 440.1 cm^3, with respective mean CTV$_{boost}$ and PTV$_{boost}$ volumes of 277.1 ± 203.1 and 438.8 ± 258.8 cm^3. Organ-at-risk dose exposure analysis data are summarized in Table 4. Bivariate linear regression modeling suggests a positive relationship of CTV and PTV volume with organ-at-risk mean dose exposure. Mean doses to right and left kidney were correlated with CTVi at R2 values of 0.3 and 0.11, and PTVi at 0.39, and 0.15, respectively. The respective R2 values for liver and spinal cord mean doses were 0.41 and 0.05 for CTVi, and 0.5 and 0.06 for PTVi. The effect of total dose prescribed was less pronounced (1% to 16%), a fact that supports the proposition that use of IMRT as the planning and delivery modality can spare critical organs and permit moderate dose escalation. Figure 6 shows linear regression plots for mean kidney doses in relation to PTV volume and total dose prescribed.

Treatment-Related Toxicity

Four patients (9.7%) were unable to complete the prescribed course of radiotherapy. One patient was prescribed chemoradiation with concurrent 5-fluorouracil (5-FU). IMRT was terminated after the patient received 46.8 Gy of the

Figure 3: Structure delineation for a BAT study displayed in an axial slice and sagittal reconstruction, as well as 3D rendering (upper figures). The lower figures show those structure outlines superimposed onto real-time acquired ultrasound images. Depicted are the mass in the pancreatic head (blue), biliary stent (red), arteries (aorta and superior mesenteric artery in orange), extrahepatic portal vein system (green), and liver outline (which is not used for alignments in pancreatic cancer) in yellow. Note that the color coding between CT simulation and BAT alignments varies. Anatomical structures are named on ultrasound images.

Table 4: Organ-at-risk dosimetric parameters.

Organ at risk	Mean dose (Gy) ±SD	Max dose (Gy) to ⅓rd ±SD	Max dose (Gy) to ⅔rds ±SD
Kidney right	16.65±5.05	12.10±4.75	17.30±5.04
Kidney left	15.49±5.14	10.97±4.48	16.29±4.81
Liver	15.2±6.82	—	—
Spinal cord	16.11±5.66	—	—

prescribed 54-Gy dose due to grade 3 upper GI toxicity including nausea, vomiting, and abdominal pain. Another patient experienced hand-foot syndrome, and treatment had to be discontinued after 30 Gy of a planned 46-Gy course. Treatment was halted in the two other patients at 54 Gy (prescribed dose 60 Gy in each case) due to a grade 4 GI bleed in one patient, and fatigue, dehydration, and worsening

performance status in the other. Five other patients had treatment interruptions lasting more than one fraction, but were able to complete the prescribed radiotherapy course.

Treatment-related toxicities are listed in Table 5. Any upper GI toxicity was experienced by 29 (70.1%) patients. The most common symptoms were nausea, vomiting, abdominal pain, and weight loss. Grades 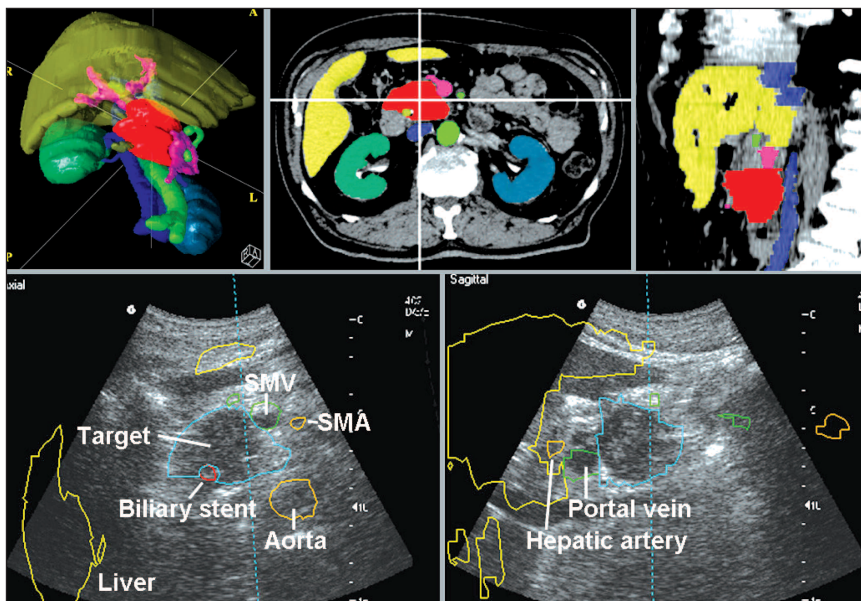1, 2, and 3 toxicity developed in 10, 16, and 3 patients, respectively. Any lower GI toxicity was reported in 17 (41.5%) patients. The most common symptom was diarrhea. Grade 1 toxicity occurred in 8 patients, grade 2 in 7 patients, and 2 patients developed grade 4 toxicity. Comparison of chemotherapy regimens (tested as gemcitabine-containing regimens vs. others) revealed no statistical correlation with observed toxicity rates or grade.

Survival Analysis

Survival data were available for all 41 patients. Separate analyses were conducted, however, for patients with a confirmed diagnosis of adenocarcinoma (n = 35) vs. other histologies (n = 6). At last follow-up (median follow-up time, 12.8 months), 8 of 35 patients with adenocarcinoma were alive (22.9%). Median overall survival in patients with adenocarcinoma was 10.3 months by Kaplan-Meier estimate, with current median survival of 18.6 months (range, 5.4–55.1 months) among patients still alive. Median estimated survival in patients with inoperable tumors was 10.0 months (range, 3.4–28.0 months). Median estimated survival in patients treated in a postoperative adjuvant setting was 10.8 months (range, 6.2–55.1 months), with 10.8 months and 10.2 months in patients with complete (R0) vs. incomplete (R1) resections. For all patients diagnosed with adenocarcinoma, 1- and 2-year actuarial survival was 38% and 25%. Figure 7 shows the respective Kaplan-Meier curves.

Median follow-up in patients with non-adenocarcinoma histologies was 17.4 months, with median survival not yet reached (range, 4.0–48.7 months; 5 of 6 patients alive at analysis).

DISCUSSION

Historically, pancreatic cancer has been associated with dismal survival outcomes. Current standard of care in the United States involves surgery and adjuvant chemoradiation.[12,13] Since only 10% to 15% of patients are resectable at the time of diagnosis,[14] treatment typically involves a multimodality approach including radiation and chemotherapy to offer palliation of symptoms. The rationale for this combination has been supported by studies that demonstrated an improvement in median survival with chemoradiotherapy vs. chemotherapy or radiotherapy alone.[15,16]

Pancreatic cancer presents a unique dilemma with regard to radiotherapeutic strategies. Treatment boundaries must adequately cover the target volume to decrease the probability of underdosing regions of microscopic disease at or near the field margins. Also, typically, the areas of recognized or probable lymphatic dissemination are included in the CTV. The location of the pancreas, contiguous with

hepatobiliary, vascular, and digestive structures, as well as its proximity to the left kidney, requires designing radiation treatment plans that minimize irradiation of adjacent dose-sensitive structures. Historically, radiation dose prescription for

Table 5: Acute treatment-related toxicity according to RTOG grading.

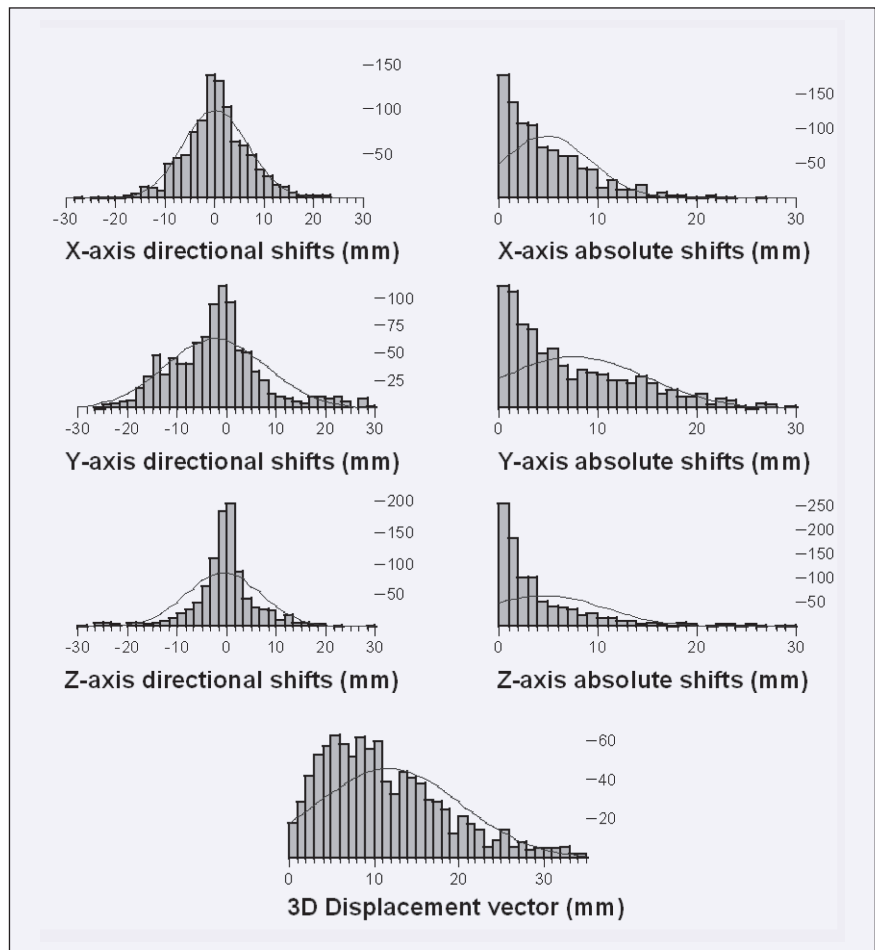| Toxicity (RTOG criteria)	Grade	n	% Patients
Upper GI	0	12	29.3
	1	10	24.4
	2	16	39.0
	3	3	7.3
	4	0	0.0
Lower GI	0	24	58.5
	1	8	19.5
	2	7	17.1
	3	0	0.0
	4	2	4.9
Maximum observed	0	9	22.0
	1	11	26.8
	2	17	41.5
	3	2	4.9
	4	2	4.9

Figure 4: Display of frequency (y-axis) of directional shifts (left figures, x-axis), and absolute shifts (right figures, x-axis) along the x-, y-, and z-axes. Fitted onto the frequency of observed length of shifts are Gaussian distributions. The lowest figure displays the frequency (y-axis) and length of the 3D magnitude vector of corrective shifts (x-axis).

pancreatic cancer has been dictated primarily by the radiotolerance of adjacent organs at risk, namely the small bowel.

Figure 5: This set of figures documents the effect of hollow organ filling on pancreatic tumor displacement recognized by ultrasound-based image guidance. The left figure shows an extended stomach at the time of original treatment CT simulation. Following consistent 3D corrective shifts >25 mm derived from ultrasound-based image guidance, the patient was re-simulated to assess the cause of shift magnitude. CT-CT comparison confirmed that the significant altered state of stomach filling had changed the target location by a calculated 3D magnitude vector of 25.1 mm (anteroposterior displacement of the displayed surgical clip 17.6 mm, left/right 6.3 mm, craniocaudally 16.7 mm). Treatment was re-planned based on the second CT scan and subsequent image guidance suggested shifts were within the range of the entire cohort.

Also, the limited radiotolerance of kidneys and the liver have required compromises in PTV coverage. Thus, radiation doses of 45.0–50.4 Gy are considered the maximally tolerated doses,[17] despite recommendations to study combined-therapy regimens with higher radiation doses.[4]

Considering the highly malignant nature of pancreatic cancer, frequent local failure, and dismal long-term survival rates, strategies to enable treatment intensification need to be developed. Radiation treatment variables that can be modified to maximize favorable outcomes include the CTV treated, options to reduce the need for PTV safety margins, and techniques to plan and deliver target volume conformal dose distributions. Realizing at least one of these parameters may allow safe escalation of radiation doses with the prospect of improved local control and survival in select patients. A fourth variable of note is dose scheduling; the body of data regarding hypofractionated and even single-dose treatments for pancreatic cancer is increasing.[18,19] These studies, however, will not be discussed in the context of the present retrospective analysis, as all data reported here refer to conventionally fractionated radiotherapy.

Involved-field radiotherapy, in which only the gross tumor volume and macroscopically enlarged lymph nodes are included in the CTV, yields a reduction of exposed tissue volume compared with a more conventional strategy of prophylactic treatment of nodal drainage stations. In an analysis of 33 patients treated with 3D-

conformal involved-field radiation to total doses of 50.0–50.4 Gy, in combination with concurrent daily cisplatin, Kawakami and co-workers documented treatment compliance in 82% and grade-3 toxicity incidences of 9% to 21%.[20] In a phase II dose-escalation trial Ceha, documented that with radiotherapy alone, doses as high as 72 Gy may be tolerated when the target volume is limited to the macroscopic tumor volume and enlarged lymph nodes.[5] While serious late effects, including fatal GI bleeding, were documented in eight patients, the authors primarily attributed their occurrence to local tumor progression.

In an effort to remediate the balance between sufficient target dose delivery and normal tissue sparing, recent data suggest that there is a decrease in small bowel irradiation and organ-at-risk radiation exposure when comparing IMRT with 3D-CRT for radiation treatment of GI malignancies.[2,3,21–23] Using IMRT as the treatment modality to deliver chemoradiation for pancreatic cancer, a favorable toxicity profile was demonstrated by Ben-Josef.[24] In a series of 15 patients treated with prescribed doses of 54 Gy to the gross tumor volume or postoperative tumor bed and 45 Gy to the nodal drainage area, one
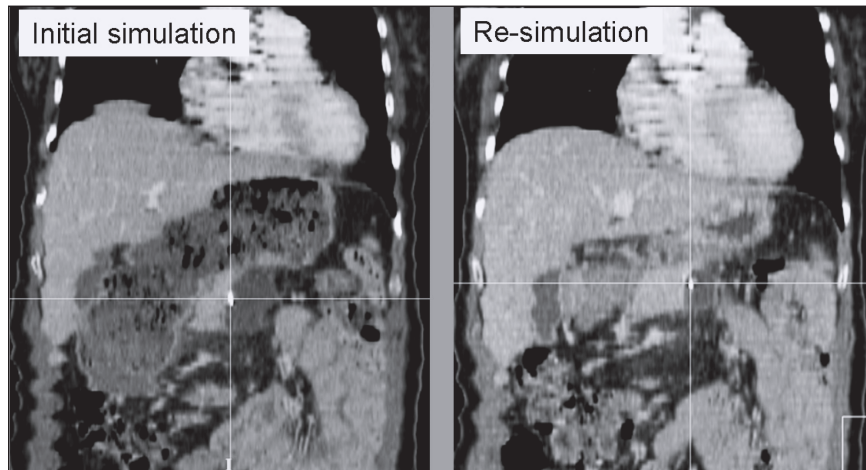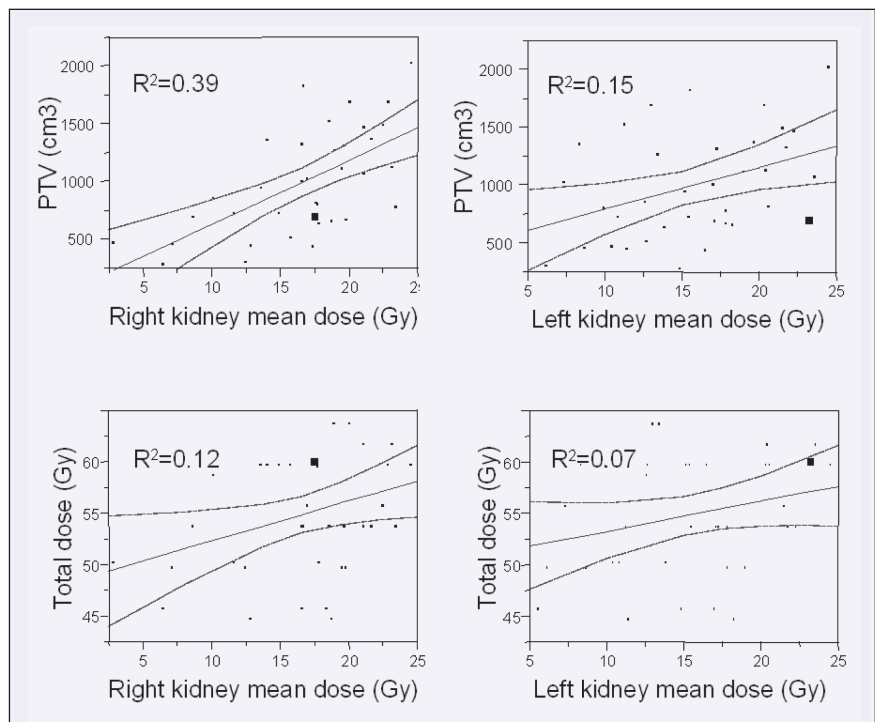

Figure 6: Linear regression plot of dose exposure of the kidneys with increasing PTVi volume and increased total prescribed dose.

patient developed a grade 3 gastric ulceration and bleeding as the most serious documented toxicity. Similarly positive experiences were reported by Milano in a series of 25 pancreatic and bile duct cancer patients treated to doses between 45.0 and 59.4 Gy to the gross tumor volume with elective nodal radiation to maximum doses of 45.0 Gy.[22] Grade 3 and 4 toxicity was observed in 5 patients, with 4 patients truncated before the full prescribed dose was delivered.

Pancreatic cancer target volume expansion into a PTV with safety margins of up to 30 mm beyond a CTV is mandated by considerable positional changes of the pancreas itself as well as the nodal drainage areas that follow organ outlines and major vascular structures. The main rationales for adding PTV marginal expansion are associated with interfraction organ motion caused by daily patient setup variations, and variations in hollow organ filling, as well as intrafraction organ motion caused predominantly by respiration.[25–27] Thus, the clinical implementation of means to ascertain target location precisely and an associated workflow to correct for setup variability online during a radiotherapy course for pancreatic cancer may enable smaller PTV safety margins without loss of target volume coverage. In this context, the term "online" refers to a positional assessment and execution of optimization of a target's location immediately prior to the respective radiation fraction actually being delivered. Such a concept must necessarily acknowledge that the component of intrafraction organ motion still must be accounted for.

Image guidance for pancreatic cancer radiotherapy can be performed using a variety of techniques. The most commonly implemented approach to image guidance, port film or electronic portal imaging (EPID), is based on the assumption that the target location is closely related to the patient's skeletal anatomy. This assumption fails in its specific application to the pancreas and nodal drainage areas, as discussed above. However, megavoltage or kilovoltage planar imaging can be useful if the target location can be marked by radiopaque fiducial markers.[28] Methods for volumetric image guidance using in-room,

diagnostic-grade CT, megavoltage CT, and on-board kilovoltage cone beam CT have recently become available. However, clinical data with respect to their application for pancreatic cancer target volumes is, as yet, unavailable.

Ultrasound has been used extensively for diagnostic assessment in the upper abdomen. Organs such as liver, kidneys, and major upper abdominal blood vessels can be reliably depicted. Additionally,
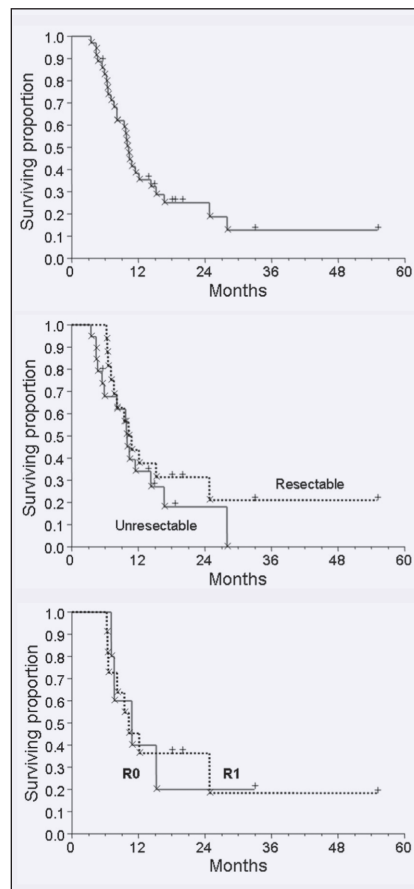

Figure 7: Kaplan-Meier actuarial survival curves for the entire cohort (top); for adjuvant radiotherapy vs. definitive radiotherapy of locally advanced disease (middle), and survival following complete vs. incomplete resection (low).

specific features of the pancreas typically can be viewed, with the head and the neck of the organ readily imaged in most patients. The pancreatic tail is more difficult to visualize. However, individually, the pancreas stands in close relationship to the aorta, celiac trunk, and superior mesenteric artery, as well as the vessels forming the extrahepatic portal vein system (Figure 3).

The authors have previously described the feasibility and workflow to use the BAT device for daily online image guidance for radiotherapy of abdominal malignancies.[8] With specific reference to pancreatic cancer, ultrasound-based image guidance may offer the ability to image the tumor directly, or reference the target location by visualizing vascular guidance structures. While the average absolute corrective shifts along the principal room axes in the present study were reasonably small (range, 4.6–7.5 mm), the 3D vector of correction exceeded 10, 20, and 30 mm in 49.9%, 27%, and 13.5% of alignments. Based on the previously published experience that ultrasound guidance was closely correlated with actual displacements based on CT-CT comparison, these corrections support the use of significant safety margins when image guidance is not employed. In return, the present data support the postulation that this form of image guidance may yield significant benefits with respect to pancreatic cancer target positioning. Most importantly, the achieved reduction in the positional variability of the target volume allows for a meaningful reduction of PTV safety margins.

It is of particular interest to contrast these data to the clinical use of PTV safety margins in recently published studies that did not specify use of daily image guidance. While a number of clinical studies accordingly employed rather large margins of up to 30 mm,[4,17,29] a relevant subset of more recently published studies report significantly smaller PTV margins of 5 mm and 10 mm for generation of a PTV.[5,18,22,30] Similarly, a virtual plan comparison study between 3D-CRT and IMRT employed 10 mm PTV safety margins.[3] The interpretation of these data must, thus, at least consider the possibility that aspects of the target might not or would not have been exposed to the prescribed dose on all scheduled treatment days.

In summary, in the present study, three variables were optimized for radiation treatment of pancreatic cancer. While the initial target volume followed more conventional guidelines and included the nodal drainage area, the boost volume was reduced to the gross tumor volume plus the area of highest risk for local tumor

recurrence. The only data available for comparison are derived from the Amsterdam high-dose radiotherapy alone study and a recent phase I radiosurgery trial.[5,28] PTVs in the first study ranged from 60–328 cm³, volumes considerably smaller than typical boost volumes in the present study. The target volumes in the radio-surgery trial were also significantly smaller, with median and maximum volumes of 29 and 72 cm³. Due to a paucity of further published data regarding actual clinical CTV and PTV volumes, the present small body of data may serve as a baseline for future clinical studies. Future target volume reduction might become reasonable by implementing magnetic resonance imaging data and molecular imaging information in the sense of a biologic target volume.

The clinical use of image guidance for pancreatic cancer was found feasible, and corrective shift data support the value of online image guidance on a daily basis. While the present experience refers to ultrasound-based image guidance only, x-ray based image-guidance assessing the location of implanted fiducial markers has been reported to be feasible for single-dose treatments of pancreatic cancer.[28] With an increasing number of on-board and in-room imaging units being delivered and becoming clinically available, volumetric image guidance may become a reasonable alternative. Supported by the 50% incidence of setup correction larger than 10 mm in the present series, daily image guidance must be employed when narrow safety margins of 10 mm or less are used to avoid the risk of uncertain dose deposition. Alternatively, so-called "no action level" strategies may be employed for unconditional corrections based on setup during the initial fractions of radiotherapy; an approach that warrants future investigation of the frequency of large random setup errors occurring throughout a course of treatment in the upper abdomen.[31,32]

IMRT planning and delivery was clinically feasible and enabled safe radiation delivery in the present series. The afforded steep dose gradients toward organs at risk allowed delivery of radiation doses to the upper end of the published range without exceeding reported toxicity rates. Organ-at-risk dose exposure in the present study was comparable with previously reported data,[22] despite the approximately 10% higher doses prescribed (50.4 vs. 55.0 Gy). While patients in the present series were treated using a serial tomotherapeutic IMRT approach, no evidence exists to reject other IMRT delivery methods, including multiple static field IMRT, as feasible alternatives. It should be noted, however, that the increased degree of freedom to deliver pencil beams over an almost full arc of rotation can only be matched by using a high number of static fields and a high-resolution multileaf collimator.

Determining the true potential for improving radiotherapy delivery for pancreatic cancer will entail the full exploration of all three variables, CTV and PTV safety margin reduction, in conjunction with state-of-the art radiotherapy planning and delivery technology. Because judicious target volume reduction can be employed using even conventional radiation delivery techniques, image guidance will benefit any mode of treatment delivery. The full potential of IMRT, however, may only be exploited when overlap between target tissues and normal tissues at risk can be minimized and the achievable steep dose gradients can only be reliably delivered when knowledge about the target's location can be obtained.

The study reported herein represents the first, but certainly not the last, effort to explore the potential and benefits of image guidance for conventionally fractionated radiotherapy of pancreatic cancer. The experiences presented and the preliminary outcomes reported support full implementation of all available technologic measures to address this disease. While preliminary survival results were within the upper third of published data for locally advanced disease, and well within the published range for adjuvant radiotherapy survival, applying the techniques presented to a more stringently selected patient population might not only provide extended preservation of their functional status and quality of life, but also yield improved local tumor control and increase the number of long-term survivors.

REFERENCES

1. Webb, S: The physical basis of IMRT and inverse planning. *Br J Radiol* 76:678-689, 2003

2. Wieland P, Dobler B, Mai S, et al: IMRT for postoperative treatment of gastric cancer: covering large target volumes in the upper abdomen: a comparison of a step-and-shoot and an arc therapy approach. *Int J Radiat Oncol Biol Phys* 59:1236-1244, 2004

3. Landry JC, Yang GY, Ting JY, et al: Treatment of pancreatic cancer tumors with intensity-modulated radiation therapy (IMRT) using the volume at risk approach (VARA): employing dose-volume histogram (DVH) and normal tissue complication probability (NTCP) to evaluate small bowel toxicity. *Med Dosim* 27:121-129, 2002

4. Abrams RA, Grochow LB, Chakravarthy A, et al: Intensified adjuvant therapy for pancreatic and periampullary adenocarcinoma: survival results and observations regarding patterns of failure, radiotherapy dose and CA19-9 levels. *Int J Radiat Oncol Biol Phys* 44:1039-1046, 1999

5. Ceha HM, van Tienhoven G, Gouma DJ, et al: Feasibility and efficacy of high dose conformal radiotherapy for patients with locally advanced pancreatic carcinoma. *Cancer* 89:2222-2229, 2000

6. Chandra A, Dong L, Huang E, et al: Experience of ultrasound-based daily prostate localization. *Int J Radiat Oncol Biol Phys* 56:436-447, 2003

7. Fuss M, Cavanaugh SX, Fuss C, et al: Daily stereotactic ultrasound prostate targeting: inter-user variability. *Technol Cancer Res Treat* 2:161-170, 2003

8. Fuss M, Salter BJ, Cavanaugh SX, et al: Daily ultrasound-based image-guided targeting for radiotherapy of upper abdominal malignancies. *Int J Radiat Oncol Biol Phys* 59:1245-1256, 2004

9. Lattanzi J, McNeeley S, Pinover W, et al: A comparison of daily CT localization to a daily ultrasound-based system in prostate cancer. *Int J Radiat Oncol Biol Phys* 43:719-725, 1999

10. Lattanzi J, McNeeley S, Hanlon A, et al: Ultrasound-based stereotactic guidance of precision conformal external beam radiation therapy in clinically localized prostate cancer. *Urology* 55:73-78, 2000

11. Mohan DS, Kupelian PA, Willoughby TR: Short-course intensity-modulated radiotherapy for localized prostate cancer with daily transabdominal ultrasound localization of the prostate gland. *Int J Radiat Oncol Biol Phys* 46:575-580, 2000

12. Yang GY, Wagner TD, Fuss M, et al: Multimodality approaches for pancreatic cancer. *CA Cancer J Clin* 55:352-367, 2005

13. Regine WF, Winter KW, Abrams R, et al. RTOG 9704: a phase III study of adjuvant pre and post chemoradiation 5-FU vs. gemcitabine for resected pancreatic adenocarcinoma. *Proc Am Soc Clin Oncol* 24:180s, 2006 (abstr 4007)

14. Yeo CJ, Cameron JL, Lillemoe KD, et al: Pancreaticoduodenectomy for cancer of the head of the pancreas. 201 patients. *Ann Surg* 221:721-731; Discussion 731-733, 1995

15. Treatment of locally unresectable carcinoma of the pancreas: comparison of combined-modality therapy (chemotherapy plus radiotherapy) to

chemotherapy alone. Gastrointestinal Tumor Study Group. *J Natl Cancer Inst* 80:751-755, 1988

16. Moertel CG, Frytak S, Hahn RG, et al: Therapy of locally unresectable pancreatic carcinoma: a randomized comparison of high dose (6000 rads) radiation alone, moderate dose radiation (4000 rads + 5-fluorouracil), and high dose radiation + 5-fluorouracil: The Gastrointestinal Tumor Study Group. *Cancer* 48:1705-1710, 1981

17. Morganti AG, Valentini V, Macchia G, et al: 5-fluorouracil-based chemoradiation in unresectable pancreatic carcinoma: phase I-II dose-escalation study. *Int J Radiat Oncol Biol Phys* 59:1454-1460, 2004

18. Allen AM, Zalupski MM, Robertson JM, et al: Adjuvant therapy in pancreatic cancer: phase I trial of radiation dose escalation with concurrent full-dose gemcitabine. *Int J Radiat Oncol Biol Phys* 59:1461-1467, 2004

19. Crane CH, Antolak JA, Rosen II, et al: Phase I study of concomitant gemcitabine and IMRT for patients with unresectable adenocarcinoma of the pancreatic head. *Int J Gastrointest Cancer* 30:123-132, 2001

20. Kawakami H, Uno T, Isobe K, et al: Toxicities and effects of involved-field irradiation with concurrent cisplatin for unresectable carcinoma of the pancreas. *Int J Radiat Oncol Biol Phys* 62:1357-1362, 2005

21. Lohr F, Dobler B, Mai S, et al: Optimization of dose distributions for adjuvant locoregional radiotherapy of gastric cancer by IMRT. *Strahlenther Onkol* 179:557-563, 2003

22. Milano MT, Chmura SJ, Garofalo MC, et al: Intensity-modulated radiotherapy in treatment of pancreatic and bile duct malignancies: toxicity and clinical outcome. *Int J Radiat Oncol Biol Phys* 59:445-453, 2004

23. Fuss M, Salter BJ, Herman TS, et al: External beam radiation therapy for hepatocellular carcinoma: potential of intensity-modulated and image-guided radiation therapy. *Gastroenterology* 127:S206-S217, 2004

24. Ben-Josef E, Shields AF, Vaishampayan U, et al: Intensity-modulated radiotherapy (IMRT) and concurrent capecitabine for pancreatic cancer. *Int J Radiat Oncol Biol Phys* 59:454-459, 2004

25. Bryan PJ, Custar S, Haaga JR, et al: Respiratory movement of the pancreas: an ultrasonic study. *J Ultrasound Med* 3:317-320, 1984

26. Horst E, Micke O, Moustakis C, et al: Conformal therapy for pancreatic cancer: variation of organ position due to gastrointestinal distention—implications for treatment planning. *Radiology* 222:681-686, 2002

27. Suramo I, Paivansalo M, Myllyla V: Cranio-caudal movements of the liver, pancreas and kidneys in respiration. *Acta Radiol Diagn* (Stockh) 25:129-131, 1984

28. Koong AC, Le QT, Ho A, et al: Phase I study of stereotactic radiosurgery in patients with locally advanced pancreatic cancer. *Int J Radiat Oncol Biol Phys* 58:1017-1021, 2004

29. Cohen SJ, Dobelbower R Jr, Lipsitz S, et al: A randomized phase III study of radiotherapy alone or with 5-fluorouracil and mitomycin-C in patients with locally advanced adenocarcinoma of the pancreas: Eastern Cooperative Oncology Group study E8282. *Int J Radiat Oncol Biol Phys* 62:1345-1350, 2005

30. Demols A, Peeters M, Polus M, et al: Adjuvant gemcitabine and concurrent continuous radiation (45 Gy) for resected pancreatic head carcinoma: a multicenter Belgian phase II study. *Int J Radiat Oncol Biol Phys* 62:1351-1356, 2005

31. Bortfeld T, van Herk M, Jiang SB: When should systematic patient positioning errors in radiotherapy be corrected? *Phys Med Biol* 47:N297-302, 2002

32. de Boer HC, Heijmen BJ: A protocol for the reduction of systematic patient setup errors with minimal portal imaging workload. *Int J Radiat Oncol Biol Phys* 50:1350-1365, 2001

Disclosures of Potential Conflicts of Interest